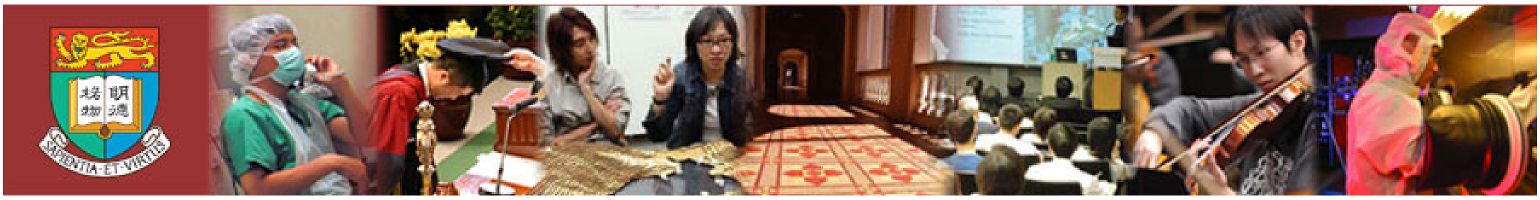

Title	Surface nitrate utilization in the Bering sea since 180kA BP: Insight from sedimentary nitrogen isotopes
Author(s)	Riethdorf, Jan Rainer; Thibodeau, Benoit; Ikehara, Minoru; Nürnberg, Dirk; Max, Lars; Tiedemann, Ralf; Yokoyama, Yusuke
Citation	Deep-Sea Research Part 2: Topical Studies in Oceanography, 2015, v. 125-126, p. 163–176
Issued Date	2015
URL	http://hdl.handle.net/10722/210587
Rights	© 2015. This manuscript version is made available under the CC-BY-NC-ND 4.0 license http://creativecommons.org/licenses/by-nc-nd/4.0/

Surface nitrate utilization in the Bering Sea since 180 ka BP: Insight from sedimentary nitrogen isotopes

Jan-Rainer Riethdorf[a,b], Benoit Thibodeau[b,c], Minoru Ikehara[d], Dirk Nürnberg[b], Lars Max[e], Ralf Tiedemann[e], and Yusuke Yokoyama[a,f]

[a]Department of Ocean Floor Geoscience, Atmosphere and Ocean Research Institute, The University of Tokyo, 5-1-5 Kashiwanoha, Kashiwa, Chiba 277-8564, Japan; jan.riethdorf@gmail.com; yokoyama@aori.u-tokyo.ac.jp

[b]Helmholtz Centre for Ocean Research Kiel (GEOMAR), Wischhofstr. 1-3, D-24148 Kiel, Germany; dnuernberg@geomar.de; bthibodeau@geomar.de

[c]Department of Chemical Oceanography, Atmosphere and Ocean Research Institute, The University of Tokyo, 5-1-5 Kashiwanoha, Kashiwa, Chiba 277-8564, Japan

[d]Center for Advanced Marine Core Research, Kochi University, B200 Monobe Nankoku, Kochi 783-8502, Japan; ikehara@kochi-u.ac.jp

[e]Alfred Wegener Institute for Polar and Marine Research, Am Handelshafen 12, D-27570 Bremerhaven, Germany; Lars.Max@awi.de; Ralf.Tiedemann@awi.de

[f]Institute of Biogeoscience, Japan Agency for Marine-Earth Science and Technology, Yokosuka 237-0061, Japan

Corresponding author and present adress:

Yusuke Yokoyama
Department of Ocean Floor Geoscience
Atmosphere and Ocean Research Institute
The University of Tokyo
5-1-5 Kashiwanoha, Kashiwa Chiba 277-8564, Japan
Mail: yokoyama@aori.u-tokyo.ac.jp
Phone: +81-4-7136-6141

Abstract

We present high-resolution records of sedimentary nitrogen ($\delta^{15}N_{bulk}$) and carbon isotope ratios ($\delta^{13}C_{bulk}$) from piston core SO201-2-85KL located in the western Bering Sea. The records reflect changes in surface nitrate utilization and terrestrial organic matter contribution in submillennial resolution that span the last 180 kyr. The $\delta^{15}N_{bulk}$ record is characterized by a minimum during the penultimate interglacial indicating low nitrate utilization (~62-80%) despite the relatively high export production inferred from opal concentrations along with a significant reduction in the terrestrial organic matter fraction (m_{terr}). This suggests that the consumption of the nitrate pool at our site was incomplete and even more reduced than today (~84%). $\delta^{15}N_{bulk}$ increases from Marine Isotope Stage (MIS) 5.4 and culminates during the Last Glacial Maximum, which indicates that nitrate utilization in the Bering Sea was raised during cold intervals (MIS 5.4, 5.2, 4) and almost complete during MIS 3 and 2 (~93-100%). This is in agreement with previous hypotheses suggesting that stronger glacial stratification reduced the nutrient supply from the subeuphotic zone, thereby increasing the iron-to-nutrient ratio and therefore the nitrate utilization in the mixed surface layer. Large variations in $\delta^{15}N_{bulk}$ were also recorded from 180 to 130 ka BP (MIS 6) indicating a potential link to insolation and sea-level forcing and its related feedbacks. Millennial-scale oscillations were observed in $\delta^{15}N_{bulk}$ and $\delta^{13}C_{bulk}$ that might be related to Greenland interstadials.

1. Introduction

The polar oceans are thought to have been more stratified during past glacial periods and the breakdown of stratification in the Southern Ocean during interglacials has been suggested as a potential control mechanism for the glacial-interglacial cycles in atmospheric carbon dioxide (CO_2) (for a review see Sigman et al., 2010). Recent studies have found supporting evidence that past variations in stratification/ventilation also occurred in the subarctic North Pacific with implications for ocean-atmosphere gas exchange (Jaccard et al., 2005, 2010; Brunelle et al., 2007, 2010; Galbraith et al., 2008a; Okazaki et al., 2010, 2012; Chikamoto et al., 2012; Menviel et al., 2012; Rella et al., 2012; Jaccard and Galbraith, 2013; Max et al., 2014).

The modern subarctic North Pacific is characterized by a permanent halocline due to a low-salinity surface layer that limits the exchange of nutrients between the surface and subsurface and prevents the formation of deep water masses (e.g., Warren, 1983; Haug et al., 1999; Emile-Geay et al., 2003). At the same time high marine productivity makes this area a net sink for atmospheric CO_2 (Honda et al., 2002; Takahashi et al., 2002b). However, the efficiency of the biological pump in the high-nutrient, low-chlorophyll (HNLC) regions of the subarctic North Pacific is reduced due to iron limitation (e.g., Tsuda et al., 2003), which results in incomplete nitrate utilization.

Sedimentary records from the North Pacific and its marginal seas consistently show reduced contents of biogenic opal and barium, $CaCO_3$, and organic carbon during past glacial periods, indicating reduced biological export production (e.g., Gorbarenko et al., 2002; Narita et al., 2002; Kienast et al., 2004; Nürnberg and Tiedemann, 2004; Jaccard et al., 2005, 2010; Okazaki et al., 2005a; Shigemitsu et al., 2007, 2008; Riethdorf et al., 2013a). Restricted marine productivity both in the North Pacific and in the Antarctic sector of the Southern Ocean is attributed to (i) light limitation due to extensive sea-ice coverage (Elderfield and Rickaby, 2000), or (ii) to enhanced stratification of the upper water column that suppressed nutrient supply to the euphotic zone (Francois et al., 1997).

Studies investigating these hypotheses applied stable nitrogen isotope ratios ($\delta^{15}N$) to provide a link to the marine nutrient cycle, but they have been mostly focused on regions not influenced by seasonal sea-ice, which has the potential to modulate biological and terrigenous fluxes. In the NW Pacific the $\delta^{15}N$ signal can be used as a proxy of surface nitrate utilization, whereas in the NE Pacific, it reflects variations in the composition of the subsurface nitrate pool (Brunelle et al., 2007; Galbraith et al., 2008a). The available reconstructions of surface nitrate utilization in the Okhotsk and Bering seas indicate that in both marginal seas enhanced stratification during glacial intervals resulted in a reduced supply of nitrate to the surface and a more complete utilization of surface nitrate because of the continued iron supply from atmospheric deposition (i.e., higher iron-to-nitrate ratio), thereby explaining the low glacial productivity (e.g., Brunelle et al., 2007, 2010; Kim et al., 2011; Khim et al., 2012).

For the Bering Sea, recent studies have found indications for millennial-scale oscillations in export production and terrigenous matter supply, which might be connected to changes in stratification and/or sea-ice influence (Gorbarenko et al., 2005, 2010b; Kim et al., 2011; Riethdorf et al., 2013a; Schlung et al., 2013). However, most of the available records of $\delta^{15}N$ are located in the southern Bering Sea and therefore not necessarily influenced by seasonal sea-ice. Moreover, the records are restricted to ~120 ka BP and do not allow for a comparison between the glacial terminations, which due to the large amplitude of climate and environmental changes are considered important periods for the understanding of the carbon cycle (e.g., Yokoyama and Esat, 2011). Especially for Marine Isotope Stage 6 (MIS 6), which in the Okhotsk Sea environment is characterized by rather extreme glacial ice conditions with significantly increased accumulation rates of ice-rafted debris (IRD) (Nürnberg et al., 2011), no records of $\delta^{15}N$ are available.

Here, we present isotope geochemical records from a supposedly sea-ice influenced site in the poorly studied western Bering Sea for the last 180 kyr in high-resolution employing sedimentary carbon and nitrogen isotope ratios to reconstruct changes in the contribution of terrestrial organic matter and surface nitrate utilization, respectively. Our results, for the first time, provide information on nitrate utilization in the Bering Sea beyond 120 ka BP and expand the hypothesis of glacial-interglacial stratification changes to cold and warm intervals. Moreover, our record suggests that millennial-scale climate oscillations occurred in the Bering Sea which might be connected to Greenland interstadials.

2. Study area

The Bering and Okhotsk seas are marginal seas of the North Pacific, separated from by the Aleutian and Kurile islands, respectively. They are bounded by the coasts of eastern Siberia, the Kamchatkan peninsula and/or western Alaska. Wide and shallow continental shelf areas are found in the northern Okhotsk and in the northern and eastern Bering Sea (Figure 1).

With respect to surface circulation, waters from the North Pacific are transported westward along the Aleutian islands by the Alaskan Stream and enter the Bering Sea via the Aleutian passes. There, the Bering Slope Current (BSC) and the East Kamchatka Current (EKC) form boundary currents (Stabeno et al., 1999). Surface outflow is directed into the Arctic through the shallow (~50 m) Bering Strait, whereas surface and deeper waters are transported back into the NW Pacific through the deeper straits, mainly Kamchatka Strait (Figure 1). The EKC and the Oyashio current flow southward and represent western boundary currents of the North Pacific subpolar gyre. The Kurile straits provide entrance and exit pathways to the Okhotsk Sea.

Major climatic and oceanographic characteristics of the North Pacific realm are the strong seasonality in sea surface temperatures (SST) and sea-ice formation, the permanent halocline, and a pronounced oxygen minimum zone (OMZ). In the Bering Sea sea-ice is present from September until July reaching its maximum distribution during March/April (Tomczak and Godfrey, 1994; Niebauer et al., 1999). Its formation is related to the interaction of the Siberian High and the Aleutian Low, which results in the advection of cold Arctic air masses, subsequent cooling of the sea surface, and strong winter mixing (Stabeno et al., 1999). Sea-ice is considered as an important transport agent of terrigenous matter in the Okhotsk and Bering seas (Nürnberg and Tiedemann, 2004; Nürnberg et al., 2011; Riethdorf et al., 2013a). Geochemical results indicate that sediments on the eastern Bering Sea shelf and in the Meiji Drift in the NW Pacific are supplied from Yukon–Bering Sea sources (VanLaningham et al., 2009; Asahara et al., 2012; Nagashima et al., 2012). Based on these results Riethdorf et al. (2013a) proposed that terrigenous matter entrained into sea-ice by tidal pumping, suspension freezing, and beach-ice formation, was transported from the eastern Bering Sea shelf to the location studied in this paper, although a contribution by suspension load carried by the BSC could not be excluded.

Although sea-ice formation and according brine rejection in the northern Okhotsk Sea drive the modern ventilation of North Pacific Intermediate Water (NPIW) (e.g., Yasuda, 1997; Yamamoto et al., 2001), the source of NPIW might have shifted to the Bering Sea in the past (Matsumoto et al., 2002; Ohkushi et al., 2003; Tanaka and Takahashi, 2005; Rella et al., 2012), where it nowadays resides at the depth of the 26.8 potential density (σ_{θ}) surface in ~200-400 m (Roden, 1995; Macdonald et al., 2001). The OMZ is found beneath the NPIW with minimum dissolved oxygen concentrations of ~15-20 μmol kg^{-1} at ~900-1100 m (Roden, 2000; Lehmann et al., 2005).

In the Bering Sea, high marine productivity is observed, which is mainly associated with shelf areas (e.g., Springer et al., 1996; Stabeno et al., 1999) and dominated by diatoms. Major biological fluxes occur during spring/summer (mainly diatoms) and late summer/early fall (coccolithophores and planktonic foraminifera) (Takahashi et al., 2002a). Nutrients are consumed during the productive seasons and returned from the subsurface by winter mixing. Although winter mixing supplies nutrients from the subsurface into the euphotic zone, near-surface nutrients are not completely consumed by phytoplankton during the productive seasons. Therefore, the western Bering Sea studied here, as well as the central eastern and western parts of the subarctic North Pacific are HNLC regions with perennially high surface nitrate concentrations (e.g., Tyrrell et al., 2005) (Figure 1). As extensively discussed in Brunelle et al. (2007, 2010) changes in the extent of surface nitrate utilization can be reconstructed using records of $\delta^{15}N$, if the underlying assumptions include a constant isotope effect for nitrate assimilation and little or no changes in the $\delta^{15}N$ of the source nitrate. There is evidence for the northward propagation of ^{15}N-enriched nitrate from the eastern tropical North Pacific along coastal North America (Liu and Kaplan, 1989; Altabet et al., 1999; Kienast et al., 2002; Sigman et al., 2003). Hence, paleoceanographic interpretations of sedimentary $\delta^{15}N$ have to consider changes in the $\delta^{15}N$ of the subsurface nitrate pool.

3. Material and methods

This study is based on 18.13 m-long piston core SO201-2-85KL (referred to as 85KL hereafter) recovered during R/V Sonne expedition SO201 KALMAR Leg 2 in 2009 (Dullo et al., 2009) from Shirshov Ridge, western Bering Sea (57°30.30'N, 170°24.77'E, 968 m deep; Figure 1). Sediments from this core mainly consist of terrigenous siliciclastic material bound to the clay- and silt-fractions, but layers of diatomaceous ooze are repeatedly intercalated. Carbonate preservation is poor and at best sporadic, and no sediments younger than 7.5 ka BP were recovered.

3.1 Bulk sedimentary analyses (TOC, TN, $\delta^{13}C_{bulk}$, $\delta^{15}N_{bulk}$)

Total organic carbon (TOC) and total nitrogen (TN) concentrations, as well as sedimentary stable carbon ($\delta^{13}C_{bulk}$) and nitrogen ($\delta^{15}N_{bulk}$) isotope ratios were determined downcore (>9.1 ka BP) every 5 cm from a total of 357 bulk sediment samples. About 25 mg of freeze-dried, hand-ground (agate mortar) sediment was weighed into Ag capsules, acidified with 100 µl hydrochloric acid (3N) to remove inorganic carbon, and dried in a desiccator filled with phosphorus(V)oxide and sodium hydroxide. To ensure complete combustion, the Ag capsules were subsequently wrapped into Sn capsules. TOC, TN, $\delta^{13}C_{bulk}$, and $\delta^{15}N_{bulk}$ were determined at the Center for Advanced Marine Core Research, Kochi University, using a Flash EA 1112 Series elemental analyzer (EA; Thermo Fisher Scientific, USA) coupled with a Delta Plus Advantage isotope ratio mass spectrometer (IRMS; Thermo Fisher Scientific, USA) via a Conflo III interface (He carrier). Stable isotope results are reported in conventional δ-notation and referenced to the Vienna PeeDee Belemnite (VPDB) standard and to atmospheric nitrogen. Molar TN/TOC ratios were corrected for inorganic nitrogen compounds based on a linear regression between TOC and TN following Goñi et al. (1998) (referred to as molar N/C ratios hereafter; Figure 2). Analytical precision (1σ) was determined from two different standards (L-Alanine, n = 58; Sulfanilamide, n = 60) and was <2% RSD (relative standard deviation) for TOC, <5% RSD for TN, ±0.01 mol mol^{-1} for N/C, ±0.14‰ for $\delta^{13}C_{bulk}$, and ±0.29‰ for $\delta^{15}N_{bulk}$. Reproducibility of the samples, determined from replicates (1σ, n = 14), was ±0.01 wt.% for TOC and TN, ±0.01 mol mol^{-1} for N/C, ±0.11‰ for $\delta^{13}C_{bulk}$, and ±0.86‰ for $\delta^{15}N_{bulk}$. This rather high value for $\delta^{15}N_{bulk}$, being significantly higher than instrumental precision, might be related to sample inhomogeneity and potential alteration of the sedimentary organic matter during pre-analysis acid treatment (Brodie et al., 2011a, 2011b).

3.2 Age model

The stratigraphic framework of 85KL is described in detail in Max et al. (2012) and Riethdorf et al. (2013a). Briefly, X-ray fluorescence (XRF) and spectrophotometric (color b*) core logging data were correlated to the $\delta^{18}O$ records of the NGRIP ice core (NGRIP members, 2004; GICC05 timescale, Rasmussen et al., 2006) and the Sanbao stalagmites (Wang et al., 2008). This approach was validated by benthic $\delta^{18}O$ stratigraphy, magnetostratigraphy, AMS ^{14}C dating of planktonic foraminifera, and intercore correlations to neighbouring sediment cores. Linear sedimentation rates vary between 4 and 23 cm kyr^{-1} (average of ~12 cm kyr^{-1}), which translates into a submillennial time-resolution for our reconstructions.

3.3 Existing data

For comparison we used logging data and geochemical results reflecting changes in export production and terrigenous matter supply already available for core 85KL. Method details are given elsewhere (Max et al., 2012; Riethdorf et al., 2013a, 2013b). In summary, light and color reflectance were measured directly after core recovery every 1 cm using a Minolta CM 508d hand-held spectrophotometer and converted into CIE L*, a*, and b* color space. XRF scanning for elements Al through to Ba was performed at 1 cm sampling resolution using the Avaatech XRF core scanner at Alfred Wegener Institute for Polar and Marine Research, Bremerhaven. Molybdate-blue spectrophotometry was used to determine biogenic opal concentrations (after Müller and Schneider, 1993), and concentrations of $CaCO_3$ were calculated from the difference of total carbon (TC) and TOC previously determined using a Carlo Erba CNS analyzer (model NA-1500) at GEOMAR, Kiel. The relative amount of siliciclastics was calculated by subtracting the sum of $CaCO_3$, TOC, and opal concentrations from a total of 100 wt.%. Records of XRF Ca/Ti log-ratios, XRF Br count rates (in counts per second, cps), and color b* correlated with $CaCO_3$ (R^2 = 0.65), TOC (R^2 = 0.64), and opal (R^2 = 0.61), respectively. This finding is in agreement with other studies linking biogenic $CaCO_3$ with normalized XRF records of Ca (Jaccard et al., 2005), TOC with biophilic Br (Ziegler et al., 2008), and opal and organic matter content with color b* (Debret et al., 2006).

3.4 Reconstruction of export production

The use of $CaCO_3$, TOC, and opal to reconstruct changes in export production is subject to specific restrictions. $CaCO_3$, especially in the North Pacific, is influenced by carbonate dissolution and might be more indicative of changes in the bottom water calcite saturation state (e.g. Jaccard et al., 2005). With respect to TOC, it is necessary to discriminate between marine and terrestrial carbon sources. The most often used proxy for reconstructions of paleo-export production in the North Pacific realm is biogenic opal (e.g. Kienast et al., 2004).

In paleoceanography, fluxes are usually reconstructed using accumulation rates rather than proxy concentrations. However, for the North Pacific and Bering Sea several studies provide evidence for the similar evolution of concentration and accumulation records of biogenic components (e.g. Crusius et al., 2004; Brunelle et al., 2007, 2010). Here, we used dry bulk density measurements (Riethdorf et al., 2013a) to calculate bulk mass accumulation rates (AR Bulk, in g cm^{-2} kyr^{-1}), as well as proxy accumulation rates for $CaCO_3$, TOC, opal, and siliciclastics. The result is shown in Figure 3, clearly demonstrating that sedimentation at Site 85KL is dominated by siliciclastic input. Overall, concentrations of the biogenic components are low, but opal concentrations and opal accumulation rates show a positive linear relationship (R^2 = 0.49). We therefore assume in this paper that at Site 85KL concentrations of opal and color b* logging data are related to export production.

4. Results

4.1 Export production and terrigenous matter supply

In general, concentrations of $CaCO_3$, TOC, and opal, as well as their approximating logging data show increased values during warm intervals (MIS 5.5, 5.3, 5.1, and 1) and Greenland interstadials (GI), but low values during cold intervals (MIS 6, 5.4, 5.2, 4, and 2) and Greenland stadials (GS) (Figure 4; Riethdorf et al., 2013a). Because of sedimentary dilution, the proxy records reflecting terrigenous matter supply (%Siliciclastics, XRF data of Al) have an inversed shape with respect to the records reflecting export production. Our EA-IRMS-based TOC results are in excellent agreement with those of Riethdorf et al. (2013a) and in higher temporal resolution extend the respective record by ~30 kyr into MIS 6. The temporal evolution of TOC recorded during MIS 6 strongly corresponds to that observed in color b*, and, to a lesser degree, in XRF Ca/Ti log-ratios and Br count rates (Figure 4). With respect to TOC concentrations, MIS 6 is characterized by a strong variability within the range of ~0.4 to ~1.7 wt.%, showing several short-lived oscillations and highest concentrations during ~156-137 ka BP.

4.2 $\delta^{13}C_{bulk}$, $\delta^{15}N_{bulk}$, N/C ratios, and estimation of the terrestrial organic matter fraction (m_{terr})

Values for $\delta^{13}C_{bulk}$ (of TOC) and for $\delta^{15}N_{bulk}$ (of TN) ranged from -25.4 to -21.9‰ and from 1.7 to 7.5‰, respectively, and N/C ratios varied between 0.04 and 0.11 mol mol^{-1} (Table 1; Figures 5 and 6). In general, $\delta^{13}C_{bulk}$ and N/C ratios are more positive during warm intervals (MIS 5.5, 5.3, 5.1, 3, and 1) and show pronounced, but short-lived maxima during GI, which especially for $\delta^{13}C_{bulk}$ exceed analytical precision and reproducibility. The cold intervals (MIS 5.4, 5.2, and 4) and some GS are characterized by decreases in both proxies. A different temporal evolution is recorded for $\delta^{15}N_{bulk}$. The base of core 85KL shows $\delta^{15}N_{bulk}$ values of ~5-6‰, which is followed by a sharp decrease at ~172 ka BP to values of ~2-3‰ (Figure 6). Subsequently, $\delta^{15}N_{bulk}$ again increases until another sudden drop of ~3‰ characterizes the transition from MIS 6 to 5.5 (Termination II). During the last interglacial $\delta^{15}N_{bulk}$ remained low at ~3‰ but it decreased even further to minimum values of 1.7‰ at the beginning of cold MIS 5.4. After MIS 5.4, a long-term trend toward higher values that continues into the early Holocene is observed. In between, increasing values were recorded during cold MIS 5.2 and 4, whereas $\delta^{15}N_{bulk}$ decreased (MIS 5.1) or remained almost constant (MIS 5.3 and 3) during warm stages. The transition from MIS 2 to 1 (Termination I) is characterized by local minima (~4-5‰) during the cold phases of Heinrich Stadial 1 (HS1; 18.0-14.7 ka BP, Sarnthein et al., 2001) and the Younger Dryas (YD; 12.9-11.7 ka BP, Blockley et al., 2012), and by an intercalated pronounced maximum during the Bølling-Allerød warm phase (B/A; 14.7-12.9 ka BP, Blockley et al., 2012) (up to 6.8‰). Subsequent to the YD, $\delta^{15}N_{bulk}$ continuously increased until highest values of 7.5‰ were recorded during the early Holocene (~10.1 ka BP). Notably, the $\delta^{15}N_{bulk}$ record also features short-lived maxima during GI, which, however, must be considered insignificant with respect to reproducibility.

Assuming that the geochemical and isotopic sedimentary composition represents a mixture of marine and terrestrial organic matter we applied a linear mixing model to estimate the fraction of terrestrial-derived organic matter (m_{terr}) using hypothetical endmember compositions. We therefore followed the results of Walinsky et al. (2009). This approach has recently been applied to a sediment core from the northern Gulf of Alaska (Addison et al., 2012). Our Holocene samples lie within the ranges reported by Smith et al. (2002) for surface sediment samples from the southeastern Bering Sea shelf, whereas our glacial samples compare to terrigenous particulate organic matter (POM) from the Yukon River (Guo and Macdonald, 2006) (Figure 5). Accordingly, we assume that the most likely organic matter sources for our site are marine phytoplankton ($\delta^{13}C$: -22 to -20‰; $\delta^{15}N$: >5‰; N/C: 0.10 to 0.15 mol mol^{-1}), soil ($\delta^{13}C$: -26.5 to -25.5‰; $\delta^{15}N$: 0 to 1‰; N/C: 0.08 to 0.10 mol mol^{-1}), and vascular plant detritus (VPD; $\delta^{13}C$: -27 to -25‰; $\delta^{15}N$: 0 to 1‰; N/C: 0 to 0.05 mol mol^{-1}) (Meyers, 1994; McQuoid et al., 2001; Geider and La Roche, 2002; Smith et al., 2002; Guo et al., 2004; Gaye-Haake et al., 2005; Guo and Macdonald, 2006; Walsh et al., 2008, and references therein) (Figure 5; Table 2). With the influence of soil considered insignificant, m_{terr} was calculated as:

$$m_{terr} = (A_{sample} - A_{mar}) / (A_{terr} - A_{mar}) \qquad \textit{(Eq. 1)}$$

In Equation 1 A refers to the $\delta^{13}C_{bulk}$ or N/C ratio of the sample and the respective average values for the assumed marine and terrestrial endmember composition summarized in Table 2. We preferred using molar N/C over C/N ratios, because mixing lines based on C/N are reported to underestimate the fraction of terrestrially derived organic carbon (Perdue and Koprivnjak, 2007). This approach resulted in similar values but in part different temporal evolutions of the respective m_{terr} records, which is attributed to the low variability in N/C ratios. m_{terr} varied between ~10% and ~90% with average values of ~40-50% (Table 1). It was lowest during warm intervals (MIS 5.5, 5.3, 5.1, 3, and 1) and GI, when marine productivity was high. Reductions of up to 50% occurred during the transitions from cold to warm intervals, whereas pronounced but short-lived increases of ~20% seem to correspond to GS (Figure 6). In the discussion we refer to m_{terr} derived from $\delta^{13}C_{bulk}$.

5. Discussion

5.1 The $\delta^{15}N_{bulk}$ signal and potential alteration

$\delta^{15}N_{bulk}$ values reflect the isotopic signature of the export flux of organic matter plus any secondary alteration of this signal during sinking and burial (e.g., Galbraith et al., 2008b; Robinson et al., 2012, and references therein). Hence, interpretation of variations in the $\delta^{15}N_{bulk}$ record must consider changes in (i) the isotopic composition of the subsurface nitrate pool, which is controlled by nitrogen fixation by diazotrophic bacteria and by denitrification, (ii) the degree of nitrification and surface nitrate utilization, and (iii) secondary alteration.

Nitrate is the primary nitrogen source for marine phytoplankton, which preferentially incorporates isotopically light (^{14}N-enriched) nitrate (Pennock et al., 1996; Waser et al., 1998). In the Bering Sea the source nitrate is supplied to the surface from below the euphotic zone with a modern value ($\delta^{15}N_{nitrate}$) of ~5.5‰ (Lehmann et al., 2005), which is slightly higher than the global deep ocean average of ~5‰ because of denitrification in the North Pacific (Sigman et al., 2000, Brunelle et al., 2007). Nitrogen fixation results in $\delta^{15}N_{nitrate}$ values that are isotopically light and close to that of air (0‰; Carpenter et al., 1997), and it is the main reason for the low $\delta^{15}N$ values of nitrate and sinking detritus in the tropical/subtropical ocean basins (e.g., Somes et al., 2010). Water column denitrification occurs under low dissolved oxygen concentrations (<5 μmol l^{-1}; Codispoti et al., 2001) and results in a ^{15}N-enriched nitrate pool (Barford et al., 1999). In this respect, $\delta^{15}N$ might also reflect redox conditions in the past with higher values during bottom water suboxia (Galbraith et al., 2004; Kashiyama et al., 2008; Jaccard and Galbraith, 2012; Robinson et al., 2012). Today, water column denitrification is mainly observed in the Arabian Sea, the eastern tropical North Pacific, and in the eastern tropical South Pacific. Thus, the export of ^{15}N-enriched waters might result in a shift toward higher $\delta^{15}N_{nitrate}$, as observed along coastal North America in the subarctic NE Pacific (Liu and Kaplan, 1989; Altabet et al., 1999; Kienast et al., 2002; Sigman et al., 2003). However, modern dissolved oxygen concentrations at Site 85KL lie above the denitrification threshold.

Results from benthic foraminiferal assemblages from the same site (Ovsepyan et al., 2013) suggest oxidizing conditions in the surface sediment layer from MIS 3 to the Last Glacial Maximum (LGM), but oxygen-depleted conditions during the mid-B/A and early Holocene. This is in agreement with Kim et al. (2011) who for Site PC23A reported on a dominance of oxic benthic foraminiferal species during MIS 2 and 3, but on dominantly dysoxic species during the B/A, early Holocene, and GI. These observations and our proxy records for export production indicate the presence of mostly oxic bottom waters and strongly reduced export of organic matter during most of the past 180 kyr, arguing against a significant impact of water column denitrification on $\delta^{15}N_{bulk}$. Over the last 180 kyr, one can expect a slightly higher $\delta^{15}N$ of nitrate during warm stages because of the greater extent of denitrification zone in the North Pacific. The isotopic impact of such increased denitrification during warm stages is thought to be relatively equal to the one observed today (~0.5‰: Lehmann et al., 2005). This shift toward heavier $\delta^{15}N$ is opposite to the expected isotopic effect of decreased nitrate utilization during interglacial scale. Thus, the relatively small increase in $\delta^{15}N_{bulk}$ during warm stages (~0.5‰) should not mask the larger isotopic variation expected from nitrate utilization change (Brunelle et al., 2007 and reference therein). Thus, we are confident that the observed variations in our $\delta^{15}N_{bulk}$ can be used to assess relative changes in the utilization of nitrate in the Bering Sea surface water except for period where dysoxia was present locally. During phases of local enhanced export production and oxygen-depleted bottom water conditions, as recorded during the B/A and the early Holocene, as well as during GI, denitrification might have resulted in a shift toward heavier $\delta^{15}N_{bulk}$ We will thus need to also consider potential changes in the ^{15}N signature of the source nitrate, therefore our nitrate utilization estimate might not be accurate during those periods and a multiproxy approach will be needed to decipher the exact cause of change in $\delta^{15}N_{bulk}$.

Nitrate utilization is incomplete in the modern subarctic North Pacific and in the Bering Sea. Accordingly, the isotopic value of the export flux of organic matter

($\delta^{15}N_{export}$) is lighter than that of $\delta^{15}N_{nitrate}$ (Altabet and Francois, 1994; Sigman et al., 1999; Needoba et al., 2003; Galbraith et al., 2008a). The difference between $\delta^{15}N_{nitrate}$ and $\delta^{15}N_{export}$ is primarily controlled by the nitrate utilization and decreases as it becomes more complete and in most of the global ocean the difference is zero due to almost complete utilization (Altabet et al., 1999; Thunell et al., 2004). We can calculate $\delta^{15}N_{export}$ for the expected integrated organic nitrogen export at Site 85KL assuming Rayleigh fractionation kinetics (Altabet and Francois, 1994; Mariotti et al., 1981) after:

$$\delta^{15}N_{export} = \delta^{15}N_{nitrate} + f / (1 - f)\ \varepsilon \ln(f) \qquad \textit{(Eq. 2)}$$

In Equation 2 f is the fraction of unutilized nitrate (i.e., $[NO_3^-]_{summer} / [NO_3^-]_{winter}$) and ε is the isotope effect for nitrate incorporation by phytoplankton, which was assumed to be constant at ~5‰ for simplification (Brunelle et al., 2007, 2010). Using a modern average for f of 0.16 (84% utilization), estimated from WOA 2009 surface nitrate concentrations (Garcia et al., 2010), gives $\delta^{15}N_{export}$ = ~3.8‰ for our site, which is 1.7‰ lower than the modern $\delta^{15}N_{nitrate}$. Unfortunately, no coretop $\delta^{15}N_{bulk}$ results are available for verification at our site.

Alternatively, secondary alteration (preferential loss of organic nitrogen, leakage of ammonium into pore waters, ammonium absorption into clay minerals, winnowing/size fractionation) might have raised the modern coretop $\delta^{15}N$ value. In general, however, alteration of the $\delta^{15}N_{bulk}$ from that of the sinking flux is not considered to have a considerable influence in organic-rich sediments from high-accumulation regions with low contributions of inorganic nitrogen compounds (for a review see Robinson et al., 2012). Core 85KL has rather high average TOC concentrations (~0.9 wt.%), whereas TIN is low at ~0.017 wt.% (Figure 2a), and the relationship between TN and $\delta^{15}N_{bulk}$ is only weak (R^2 = 0.24; Figure 2b), which argues against alteration. Moreover, in comparison with other Bering Sea records using $\delta^{15}N$ as a proxy for nitrate utilization (Brunelle et al., 2007, 2010; Kim et al., 2011; Schlung et al., 2013) our $\delta^{15}N_{bulk}$ record generally shows a similar evolution (Figure 7). Notably, at our study site $\delta^{15}N_{bulk}$ values >5.5‰ were mainly recorded during Termination I, which, in accordance with the previously mentioned studies is more likely attributed to enhanced deglacial water column denitrification.

Finally, there might have been influence from terrestrial nitrogen, since our estimates for m_{terr} suggest significant average contributions (~40-50%) of terrestrial organic matter in Shirshov Ridge sediments. In this respect, variations in $\delta^{15}N_{bulk}$ might reflect changes in the supply of terrestrial nitrogen. However, for the estimation of m_{terr} we assumed that the $\delta^{15}N_{bulk}$ of terrestrial organic matter is lower than that of marine organic matter. If there was considerable influence from terrestrial nitrogen we would expect a strong positive relationship between N/C ratios and $\delta^{15}N_{bulk}$, which is not observed (R^2 = 0.10). Accordingly, although Site 85KL is characterized by overall high m_{terr} values with a strong downcore variability, there seems to have been no significant influence of m_{terr} on the $\delta^{15}N_{bulk}$ signal, which might be explained by an only low fraction of terrestrial nitrogen. We therefore consider the influence of secondary alteration and contamination from terrestrial nitrogen on the $\delta^{15}N_{bulk}$ signal as insignificant and in the following discuss variations in $\delta^{15}N_{bulk}$ by means of changes in surface nitrate utilization.

5.2 Cold and warm intervals of the past 180 kyr

At Site 85KL, glacial periods, specifically cold intervals (MIS 6, 5.4, 5.2, and 4 to 2), were characterized by significantly reduced export production and enhanced terrigenous matter supply (Riethdorf et al., 2013a; Figure 4), which is in agreement with other studies from the subarctic North Pacific (e.g., Kienast et al., 2004; Jaccard et al., 2005), the Okhotsk Sea (e.g., Narita et al., 2002; Nürnberg and Tiedemann, 2004; Okazaki et al., 2005b; Nürnberg et al., 2011), and the Bering Sea (e.g., Okazaki et al., 2005a; Brunelle et al., 2007; Kim et al., 2011). This is supported by our reconstruction of m_{terr} indicating an average terrestrial organic matter fraction of ~40-50%, which is significantly reduced only during warm intervals. Today, the organic matter in Bering Sea sediments is dominantly of marine origin (Méheust et al., 2013). The glacial terrigenous matter source of Bering Sea sediments is under debate, but there are indications that they originate from source rocks drained by the Yukon River (VanLaningham et al., 2009), and/or from sea-ice rafting in the NE Bering Sea (Riethdorf et al., 2013a).

For the Bering and Okhotsk seas the outlined observations were explained by enhanced sea-ice influence and stronger stratification of the upper water column during cold climate conditions restricting marine productivity (Nürnberg and Tiedemann, 2004; Brunelle et al., 2007, 2010; Kim et al., 2011; Khim et al., 2012; Riethdorf et al., 2013a). This restriction results from the extended sea-ice season and coverage and the subsequent limitation of light availability and vertical mixing (nutrient supply), but temperature limitation is likely to have played an additional role. An extended Bering Sea sea-ice coverage during cold phases is supported by reconstructions from diatom assemblages (Katsuki and Takahashi, 2005) and from the diatom-derived, highly branched isoprenoid sea ice biomarker (IP_{25}) (Max et al., 2012).

Records of sedimentary and diatom-bound $\delta^{15}N$ imply enhanced surface nitrate utilization as a result of stronger upper water column stratification in the Bering Sea, especially during MIS 3 and 2 (Brunelle et al., 2007, 2010; Kim et al., 2011). Similar observations are reported for the Okhotsk Sea (Brunelle et al., 2010; Khim et al., 2012) and the subarctic NW Pacific (Galbraith et al., 2008a; Brunelle et al., 2010), indicating that these regions were not always HNLC. This shift towards higher $\delta^{15}N$ in MIS 3 is, however, not observed at IODP Site U1340 at the northeastern flank of Bowers Ridge (Schlung et al., 2013). Instead, a sharp decrease in $\delta^{15}N_{bulk}$ was recorded at this site at ~55 ka BP, which might be related to local stratification changes, or to the influence of turbidites that are reported to compromise records recovered from that area (Nakatsuka et al., 1995). Our $\delta^{15}N_{bulk}$ results are in accordance with the former Bering Sea studies confirming enhanced nitrate utilization during cold intervals, but they seem to reveal a more complex development of stratification and for the first time provide information for MIS 6:

At the base of core 85KL (~180-173 ka BP), early MIS 6 is characterized by high $\delta^{15}N_{bulk}$ values indicating almost complete nitrate utilization, when export production was reduced, but maintained. Relatively high $\delta^{15}N_{bulk}$ during MIS 6 were also recorded at Okhotsk Sea sites GGC27 (Brunelle et al., 2010) and GC9A (Khim et al., 2012), as well as at ODP Site 882 and at Site MD01-2416 (Galbraith et al., 2008a). Hence, low insolation and weak seasonal contrasts most probably caused a prolonged sea-ice season, extended sea-ice coverage, and suppressed vertical mixing. At ~172 ka BP, when Northern Hemisphere summer insolation had a local maximum, a sharp decrease in $\delta^{15}N_{bulk}$ implies a sudden drop in nitrate utilization (from ~100% to ~50-70%) in the Bering Sea (Figure 6). At the same time export production was increased, whereas m_{terr} decreased. This might be explained by a shortened sea-ice season, reduced sea-ice coverage, and enhanced winter mixing due to stronger seasonal contrasts, which increased the nutrient supply from the subeuphotic zone.

Accordingly, we speculate that changes in nitrate utilization are strongly affected by insolation forcing and a feedback by sea-ice processes that drive the extent of vertical mixing during winter, as well as the input of terrestrial organic matter. Dominant climate control via insolation has already been proposed for the Okhotsk Sea (Gorbarenko et al., 2010a, 2012). The long-term increase in nitrate utilization after ~172 ka BP until Termination II, which is also observed at the Okhotsk Sea and NW Pacific sites (Figure 7), as well as the long-term increase from MIS 5.4 until Termination I might be explained by increasingly fostered stratification (i.e. a reduction in the supply of nutrients into the euphotic zone), which is finally subject to a 'breakdown' during the deglaciations. It is beyond the scope of this paper to decipher the underlying causes of this deglacial breakdown, but increasing insolation resulting in a reduced sea-ice season and strengthened winter mixing, is a likely contributing factor.

The observation that the strongest maxima in Northern Hemisphere summer insolation, mainly those of warm intervals (MIS 5.5, 5.3, 5.1, and 1), are reflected by maxima in export production (Figure 4), minima in m_{terr}, and decreasing or constant $\delta^{15}N_{bulk}$ (Figure 6), supports the view that insolation changes affect nutrient-limited marine productivity by a feedback in sea-ice processes and winter mixing. It is also in agreement with previously published concepts proposed to explain glacial-interglacial changes in the Okhotsk (Seki et al., 2004; Okazaki et al., 2005b; Khim et al., 2012) and Bering seas (Nakatsuka et al., 1995; Kim et al., 2011). When applying Equation 2, our $\delta^{15}N_{bulk}$ record indicates increasing nitrate utilization during cold MIS 5.4 (from ~50 to ~90%), MIS 5.2 (from ~90 to ~100%), and MIS 4 (from ~80 to ~93%), and almost complete utilization during MIS 3 and 2 (~93-100%). On the other hand, decreasing or constant nitrate utilization was recorded during warm MIS 5.5 (from ~97 to ~62%), MIS 5.3 (~90%), and MIS 5.1 (from ~100 to ~80%). This suggests that stratification was fostered during cold intervals, but weakened during warm intervals due to the processes outlined above.

The low glacial $\delta^{15}N_{bulk}$ values of ~2-3‰ at the beginning of MIS 5.4, of ~3.5-4.5‰ at the beginning of MIS 4, and the concurrent increases in m_{terr} (Figure 6) might be explained (i) by a higher contribution of (^{15}N-depleted) terrestrial organic matter, or (ii) by stronger vertical mixing. We disregard the first possibility, because we already discarded the potential effect of terrestrial nitrogen on the $\delta^{15}N_{bulk}$ signal (Section 5.1). Stronger vertical mixing in the Bering Sea during MIS 5.4 and 4 might be related to the increased formation and/or ventilation of intermediate waters as inferred from neodymium isotope ratios by Horikawa et al. (2010). The authors suggested that sea-ice formation and according brine rejection led to the subduction of surface waters to intermediate depths. Enhanced formation of sea-ice, acting as the transport agent for terrestrial organic matter would be in accordance with this assumption and explain the higher m_{terr} values. Other studies support the idea of well-ventilated intermediate waters in the Bering Sea and North Pacific during glacial times (Ohkushi et al., 2003; Itaki et al., 2009; Kim et al., 2011) and during severe stadial episodes (Rella et al., 2012). The enhanced formation and/or ventilation of intermediate waters at the end of MIS 6 and during the LGM implied by the record of Horikawa et al. (2010) is not reflected in our $\delta^{15}N_{bulk}$ record, which rather suggests strong stratification during that time. However, these observations are not necessarily contradictory, since intermediate waters could have been formed outside the still-stratified Bering Sea. In fact, recent reconstructions of past ventilation changes in the subarctic North Pacific using radiocarbon-derived ventilation ages in combination with epibenthic stable carbon isotope ratios point to the Okhotsk Sea as the source region of intermediate waters during HS1 and the YD (Max et al., 2014).

In addition to insolation forcing, sea-level changes might have influenced the extent of stratification in the Bering Sea. Today, the only shallow (~50 m) Bering Strait allows for oceanic communication between the North Pacific and the N Atlantic. During glacial times the closed Bering Strait prevented the flux of relatively fresh waters into the Atlantic, which is thought to have affected the Atlantic meridional overturning circulation (Hu et al., 2010). Lower glacial sea-level is also likely to have reduced the inflow of Alaskan Stream waters into the Bering Sea (Gorbarenko et al., 2005; Tanaka and Takahashi, 2005). As suggested by relative sea-level reconstructions (e.g., Waelbroeck et al., 2002; Yokoyama and Esat, 2011), the Bering Strait was closed during MIS 6 and in between MIS 4 to 2 until ~12-11 ka BP (Keigwin et al., 2006) (Figure 6). Our $\delta^{15}N_{bulk}$ values indicate almost complete nitrate utilization during late MIS 6 (~150-130 ka BP) and during MIS 3 and 2 as a result of strong stratification. During this time a closed Bering Strait is likely to have fostered stratification due to the pooling of the relatively fresh waters within the Bering Sea, which would have resulted in a strengthened pycnocline. Support for this view and for fresher glacial conditions in the Bering Sea comes from diatom and radiolarian assemblages (Sancetta, 1983; Katsuki and Takahashi, 2005; Tanaka and Takahashi, 2005). Notably, during MIS 3 and 2 the $\delta^{15}N_{bulk}$ values recorded at Shirshov Ridge are on average ~1‰ lower than at Bowers Ridge Site 17JPC and ~0.5‰ lower than at Site PC24A (Figure 7). This might indicate that stratification in the Bering Sea was regionally different and more pronounced in the South, or that influence from denitrification resulted in the heavier $\delta^{15}N$ values.

5.3 Deglacial and interglacial conditions

In our records, the deglaciations are characterized by the transition from the glacial situation of pronounced stratification with almost complete nitrate utilization and low export production toward the interglacial situation of reduced stratification, high marine productivity, and reduced terrestrial input. Yet, Termination II and Termination I show some notable differences. During Termination I our $\delta^{15}N_{bulk}$ record is characterized by an initial decrease, which might correspond to the HS1 cold phase, subsequent local maxima during the B/A and the early Holocene warm phases, and an intercalated minimum during the YD (Figure 6). The same temporal evolution was reported for sedimentary and diatom-bound $\delta^{15}N$ at Bering Sea sites 17JPC (Brunelle et al., 2007, 2010) and PC24A (Kim et al., 2011). The B/A-peak, occurring simultaneously with a rise in export production, is found in several other records from the North Pacific realm and related to enhanced denitrification (Keigwin et al., 1992;

Emmer and Thunell, 2000; Ternois et al., 2001; Kienast et al., 2002; Galbraith et al., 2008a; Kao et al., 2008; Brunelle et al., 2007, 2010; Addison et al., 2012; Khim et al., 2012; Schlung et al., 2013).

Notably, m_{terr} shows a local maximum during HS1 at Site 85KL. Hence, the initial decrease in $\delta^{15}N_{bulk}$ might be related to higher terrestrial input or to lower nitrate utilization due to weakened stratification. However, the latter should have resulted in higher export production, which is not observed at our site. This drop is not fully understood and alternative explanations include changes in $\delta^{15}N_{nitrate}$, iron limitation, and light limitation (Brunelle et al., 2007, 2010; Lam et al., 2013). Light limitation by expanded sea-ice coverage is supported by the qualitative detection of IP_{25} in western Bering Sea sediments during HS1 and the YD (Max et al., 2012).

During the B/A and the early Holocene our $\delta^{15}N_{bulk}$ values exceeded the modern $\delta^{15}N_{nitrate}$ value, supporting an increase in denitrification. At the same time a shift toward oxygen-depleted bottom water conditions is inferred from benthic foraminiferal assemblages (Kim et al., 2011; Ovsepyan et al., 2013), which is in agreement with the proposed expansion of the OMZ and the occurrence of laminated sediments during warm intervals (e.g., Zheng et al., 2000; van Geen et al., 2003; Cook et al., 2005). A recent comparison between alkenone- and Mg/Ca-based paleotemperature estimates suggests enhanced thermal mixed-layer stratification in the western Bering Sea during the B/A (Riethdorf et al., 2013b), implying that at least some of the recorded $\delta^{15}N_{bulk}$ increase is due to stronger surface nitrate utilization. Recently, Lam et al. (2013) suggested two stepwise events starting with deep convection initialized at ~18 ka BP increasing the nutrient supply but inducing light limitation, and subsequent meltwater-induced stratification resulting in bloom conditions and leaving surface waters enriched in nutrients. The drop in $\delta^{15}N_{bulk}$ observed during the YD in hand with decreasing SSTs and the presence of IP_{25} (Max et al., 2012) argues for a similar situation as recorded during HS1.

Termination II differs from Termination I at Site 85KL in such that the $\delta^{15}N_{bulk}$ values are lower and presumably not affected by denitrification. An early deglacial $\delta^{15}N_{bulk}$ minimum at ~133 ka BP, followed by a local maximum at ~131 ka BP might hint toward analogs of the HS1 and the B/A, respectively. The subsequent drop in $\delta^{15}N_{bulk}$

into MIS 5.5 reflecting the 'breakdown' of glacial stratification is sudden and accompanied by the decrease in both, m_{terr} and bottom water oxygenation then prevailing during the penultimate interglacial (Figure 6). Notably, this drop from relatively high MIS 6 values occurred ~5 kyr before the maximum in insolation was reached, but its timing is comparable to that recorded in the NW Pacific. In the Okhotsk Sea it seems to have occurred significantly earlier at ~147-141 ka BP (Figure 7). A respective drop in $\delta^{15}N_{bulk}$ during Termination I was not recorded at Site 85KL until ~9.1 ka BP, while at Bowers Ridge sites U1340 (Schlung et al., 2013) and 17JPC (Brunelle et al., 2007) it occurred directly after the B/A maximum.

5.4 Millennial-scale oscillations

Riethdorf et al. (2013a) reported on millennial-scale oscillations in core 85KL, thought to reflect increased export production and sudden sea-ice melt, which might be connected to GI (Dansgaard-Oeschger events; e.g., Dansgaard et al., 1993). Similar observations are reported for other sediment cores from the Bering Sea (Gorbarenko et al., 2005, 2010b; Kim et al., 2011; Rella et al., 2012; Schlung et al., 2013) and the Okhotsk Sea (Gorbarenko et al., 2007, 2010a, 2012), indicating warmer SSTs, enhanced marine productivity, weak ventilation of intermediate waters, and poor (dysoxic) dissolved oxygen conditions during interstadials. NE Pacific sediments related to GI are in part laminated and suggested to reflect phases of weak ventilation of NPIW and fluctuations in the strength of the OMZ (Behl and Kennett, 1996; Cannariato and Kennett, 1999; Hendy and Kennett, 2000, 2003). Results of Ortiz et al. (2004) from a core off Baja California implied that elevated marine productivity was caused by enhanced nutrient flux to surface waters.

In the Bering Sea higher interstadial $\delta^{15}N_{bulk}$ values were explained by Kim et al. (2011) by increased marine productivity as a result of reduced sea-ice influence and a strengthened BSC. They also suggested that stronger inflow of water masses from the Gulf of Alaska (Gorbarenko et al., 2005) resulted in enhanced nutrient supply to Bering Sea surface waters. Schlung et al. (2013) attributed higher $\delta^{15}N_{bulk}$ and concurrent minima in planktonic $\delta^{13}C$ to amplified local upwelling of subsurface nitrate rather than to increased nitrate utilization. Our data show short-lived maxima in $\delta^{15}N_{bulk}$ and concurrent minima in m_{terr} during some, but not all, GI (1, 7, 8, 12, 17-20), and during MIS 6 (at ~133, ~148, and ~173 ka BP) when export production was high (Figure 6). The opposite pattern was recorded when export production was low during some GS (2, 7, 18, 20) and also during MIS 6 (at ~151, ~157, and ~170 ka BP). Despite the low reproducibility of our $\delta^{15}N_{bulk}$ results our data support the view of increased interstadial marine productivity which led to stronger utilization of the available nitrate in a still stratified upper water column. During interstadials warmer SSTs most probably resulted in less sea-ice influence and reduced supply of terrestrial organic matter. Conversely, during stadials strengthened sea-ice formation and coverage is likely to have restricted marine productivity, led to enhanced terrestrial organic matter supply to Bering Sea sediments, and resulted in better ventilation of NPIW, potentially making the Bering Sea a proximate source of this water mass as suggested by Rella et al. (2012).

6. Summary

We determined TN, TOC, $\delta^{13}C_{bulk}$ and $\delta^{15}N_{bulk}$ in a core from the western Bering Sea in high-resolution to reconstruct changes in surface nitrate utilization (stratification) over the last 180 kyr. A linear endmember model was applied to assess the contributions of marine- and terrestrial-derived organic matter. Besides the expected difference between glacial and interglacial conditions reported for the subarctic NW Pacific and its marginal seas, our results suggest a more complex evolution of stratification with enhanced vertical mixing during warm intervals (MIS 5.5, 5.3, 5.1, 1), and stratification becoming fostered during cold intervals (MIS 6, 5.4, 5.2, 4-2). This development is explained by insolation forcing and a feedback in sea-ice formation and the strength of winter mixing. In addition, sea-level changes might have further influenced the extent of stratification when the Bering Strait was closed and relatively fresh waters pooled in the Bering Sea. During warm intervals, variations in seasonal contrasts, sea-ice influence, and stratification resulted in enhanced export production and dominantly marine-derived organic matter, but less nitrate utilization due to better vertical mixing. Conversely, enhanced terrestrial-derived organic matter, most probably associated with sea-ice formation, low export production, and enhanced stratification characterized cold intervals of the past 180 kyr. Moreover, we present supporting evidence that millennial-scale climate oscillations connected with Greenland interstadials occurred in the Bering Sea environment, and that sea-ice formation there influenced the ventilation of North Pacific Intermediate Water.

Acknowledgements

Financial support for this study was provided by a Japan Society for the Promotion of Science (JSPS) short-term postdoctoral fellowship to J.-R.R. (grant no. PE12528). Additional support came from the "Funding Program for Next Generation World-Leading Researchers (NEXT Program GR031)" of JSPS, initiated by the Council for Science and Technology Policy (CSTP), awarded to Y.Y. Core 85KL was recovered in the framework of the joint German-Russian research project KALMAR, funded by the German Federal Ministry of Education and Research (BMBF, grant nos. 03G0672A and B). We thank N. Ohkouchi, N. Harada, Y. Okazaki, and H. Vollstaedt for helpful discussions, as well as Christina Ravelo and the anonymous reviewer for their fruitful comments that improved the manuscript. Supplementary data are available via the PANGAEA Data Publisher for Earth & Environmental Science (http://doi.pangaea.de/10.1594/PANGAEA.807383).

References

Addison, J.A., Finney, B.P., Dean, W.E., Davies, M.H., Mix, A.C., Stoner, J.S., Jaeger, J.M., 2012. Productivity and sedimentary $\delta^{15}N$ variability for the last 17,000 years along the northern Gulf of Alaska. Paleoceanography 27, PA1206. doi:10.1029/2011PA002161.

Altabet, M.A., Francois, R., 1994. Sedimentary nitrogen isotopic ratio as a recorded for surface ocean nitrate utilization. Global Biogeochem. Cy. 8 (1), 103-116.

Altabet, M.A., Pilskaln, C., Thunell, R., Pride, C., Sigman, D., Chavez, F., Francois, R., 1999. The nitrogen isotope biogeochemistry of sinking particles from the margin of the Eastern North Pacific. Deep-Sea Res. Pt. I 46, 655-679.

Asahara, Y., Takeuchi, F., Nagashima, K., Harada, N., Yamamoto, K., Oguri, K., Tadai, O., 2012. Provenance of terrigenous detritus of the surface sediments in the Bering and Chukchi Seas as derived from Sr and Nd isotopes: Implications for recent climate change in the Arctic regions. Deep-Sea Res. Pt. II 61-64, 155-171. doi:10.1016/j.dsr2.2011.12.004.

Barford, C.C., Montoya, J.P., Altabet, M.A., Mitchell, R., 1999. Steady-state nitrogen isotope effects of N_2 and N_2O production in *Paracoccus denitrificans*. Appl. Environ. Microb. 65 (3), 989-994.

Behl, R.J., Kennett, J.P., 1996. Brief interstadial events in the Santa Barbara basin, NE Pacific, during the past 60 kyr. Nature 379, 243-246.

Blockley, S.P.E., Lane, C.S., Hardiman, M., Rasmussen, S.O., Seierstad, I.K., Steffensen, J.P., Svensson, A., Lotter, A.F., Turney, C.S.M., Ramsey, C.B., INTIMATE members, 2012. Synchronisation of palaeoenvironmental records over the last 60,000 years, and an extended INTIMATE event stratigraphy to 48,000 b2k. Quaternary Sci. Rev. 36, 2-10. doi:10.1016/j.quascirev.2011.09.017.

Brodie, C.R., Casford, J.S.L., Lloyd, J.M., Leng, M.J., Heaton, T.H.E., Kendrick, C.P., Yongqiang, Z., 2011a. Evidence for bias in C/N, $\delta^{13}C$ and $\delta^{15}N$ values of bulk organic matter, and on environmental interpretation, from a lake sedimentary sequence by pre-analysis acid treatment methods. Quaternary Sci. Rev. 30, 3076-3087. doi:10.1016/j.quascirev.2011.07.003.

Brodie, C.R., Heaton, T.H.E., Leng, M.J., Kendrick, C.P., Casford, J.S.L., Lloyd, J.M., 2011b. Evidence for bias in measured $\delta^{15}N$ values of terrestrial and aquatic organic materials due to pre-analysis acid treatment methods. Rapid Commun. Mass Sp. 25, 1089-1099. doi:10.1002/rcm.4970.

Brunelle, B.G., Sigman, D.M., Cook, M.S., Keigwin, L.D., Haug, G.H., Plessen, B., Schettler, G., Jaccard, S.L., 2007. Evidence from diatom-bound nitrogen isotopes for subarctic Pacific stratification during the last ice age and a link to North Pacific denitrification changes. Paleoceanography 22, PA1215. doi:10.1029/2005PA001205.

Brunelle, B.G., Sigman, D.S., Jaccard, S.L., Keigwin, L.D., Plessen, B., Schettler, G., Cook, M.S., Haug, G.H., 2010. Glacial/interglacial changes in nutrient supply and stratification in the western subarctic North Pacific since the penultimate glacial maximum. Quaternary Sci. Rev. 29, 2579-2590. doi:10.1016/j.quascirev.2010.03.010.

Cannariato, K.G., Kennett, J.P., 1999. Climatically related millennial-scale fluctuations in strength of California margin oxygen-minimum zone during the past 60 k.y.. Geology 27 (11), 975-978.

Carpenter, E.J., Harvey, H.R., Fry, B., Capone, D.G., 1997. Biogeochemical tracers of the marine cyanobacterium *Trichodesmium*. Deep-Sea Res. Pt. I 44 (1), 27-38.

Chikamoto, M.O., Menviel, L., Abe-Ouchi, A., Ohgaito, R., Timmermann, A., Okazaki, Y., Harada, N., Oka, A., Mouchet, A., 2012. Variability in North Pacific intermediate and deep water ventilation during Heinrich events in two coupled climate models. Deep-Sea Res. Pt. II 61-64, 114-126. doi:10.1016/j.dsr2.2011.12.002.

Codispoti, L.A., Brandes, J.A., Christensen, J.P., Devol, A.H., Naqvi, S.W.A., Paerl, H.W., Yoshinari, T., 2001. The oceanic fixed nitrogen and nitrous oxide budgets: Moving targets as we enter the anthropocene?. Sci. Mar. 65 (Suppl. 2), 85-105.

Cook, M.S., Keigwin, L.D., Sancetta, C.A., 2005. The deglacial history of surface and intermediate water of the Bering Sea. Deep-Sea Res. Pt. II 52, 2163-2173. doi:10.1016/j.dsr2.2005.07.004.

Crusius, J., Pedersen, T.F., Kienast, S., Keigwin, L., Labeyrie, L., 2004. Influence of northwest Pacific productivity on North Pacific Intermediate Water oxygen concentrations during the Bolling-Allerod interval (14.7--12.9 ka). Geology 32 (7), 633-363. doi: 10.1130/G20508.1.

Dansgaard, W., Johnsen, S.J., Clausen, H.B., Dahl-Jensen, D., Gundestrup, N.S., Hammer, C.U., Hvidberg, C.S., Steffensen, J.P., Sveinbjörnsdottir, A.E., Jouzel, J., Bond, G., 1993. Evidence for general instability of past climate from a 250-kyr ice-core record. Nature 364, 218-220.

Debret, M., Desmet, M., Balsam, W., Copard, Y., Francus, P., Laj, C., 2006. Spectrophotometer analysis of Holocene sediments from an anoxic fjord: Saanich Inlet, British Columbia, Canada. Mar. Geol. 229, 15-28. doi:10.1016/j.margeo.2006.01.005.

Dullo, W.-C., Baranov, B., van den Bogaard, C. (Eds.), 2009. FS Sonne Fahrtbericht/Cruise Report SO201-2 KALMAR, Busan/Korea-Tomakomai/Japan, 30.08.-08.10.2009. IFM-GEOMAR Report 35, Leibniz Institute of Marine Sciences, Kiel, 233 pp.

Elderfield, H., Rickaby, R.E.M., 2000. Oceanic Cd/P ratio and nutrient utilization in the glacial Southern Ocean. Nature 405, 305-310.

Emile-Geay, J., Cane, M., Naik, N., Seager, R., Clement, A.C., van Geen, A., 2003. Warren revisited: Atmospheric freshwater fluxes and "Why is no deep water formed in the North Pacific". J. Geophys. Res. 108 (C6), 3178. doi:10.1029/2011JC001058.

Emmer, E., Thunell, R.C., 2000. Nitrogen isotope variations in Santa Barbara Basin sediments: Implications for denitrification in the eastern tropical North Pacific during the last 50,000 years. Paleoceanography 15 (4), 377-387. doi:10.1029/1999PA000417.

Francois, R., Altabet, M.A., Yu, E.-F., Sigman, D.M., Bacon, M.P., Frank, M., Bohrmann, G., Bareille, G., Labeyrie, L.D., 1997. Contribution of Southern Ocean surface-water stratification to low atmosphere CO_2 concentrations during the last glacial period. Nature 389, 929-935.

Galbraith, E.D., Kienast, M., Pedersen, T.F., Calvert, S.E., 2004. Glacial-interglacial modulation of the marine nitrogen cycle by high-latitude O_2 supply to the global thermocline. Paleoceanography 19, PA4007. doi:10.1029/2003PA001000.

Galbraith, E.D., Kienast, M., Jaccard, S.L., Pedersen, T.F., Brunelle, B.G., Sigman, D.M., Kiefer, T., 2008a. Consistent relationship between global climate and surface nitrate utilization in the western subarctic Pacific throughout the last 500 ka. Paleoceanography 23, PA2212. doi:10.1029/2007PA001518.

Galbraith, E.D., Sigman, D.M., Robinson, R.S., Pedersen, T.F., 2008b. Nitrogen in past marine environments, in: Capone, D.G., Bronk, D.A., Mulholland, M.R., Carpenter, E.J. (Eds.), Nitrogen in the Marine Environment. Second Edition, Elsevier Inc., pp. 1497-1535. doi:10.1016/B978-0-12-372522-6.00034-7.

Garcia, H.E., Locarnini, R.A., Boyer, T.P., Antonov, J.I., 2010. World Ocean Atlas 2009, Volume 4: Nutrients (phosphate, nitrate, and silicate), in: Levitus, S. (Ed.), NOAA Atlas NESDIS 71. U.S. Government Printing Office, Washington, D.C., 184 pp.

Gaye-Haake, B., Lahajnar, N., Emeis, K.-Ch., Unger, D., Rixen, T., Suthhof, A., Ramaswamy, V., Schulz, H., Paropkari, A.L., Guptha, M.V.S., Ittekkot, V., 2005. Stable nitrogen isotopic ratios of sinking particles and sediments from the northern Indian Ocean. Mar. Chem. 96, 243-255. doi:10.1016/j.marchem.2005.02.001.

Geider, R.J., La Roche, J., 2002. Redfield revisited: variability of C:N:P in marine microalgae and its biochemical basis. Eur. J. Phycol. 37, 1-17. doi:10.1017/S0967026201003456.

Goñi, M.A., Ruttenberg, K.C., Eglinton, T.I., 1998. A reassessment of the sources and importance of land-derived organic matter in surface sediments from the Gulf of Mexico. Geochim. Cosmochim. Ac. 62 (18), 3055-3075.

Gorbarenko, S.A., Khusid, T.A., Basov, I.A., Oba, T., Southon, J.R., Koizumi, I., 2002. Glacial Holocene environment of the southeastern Okhotsk Sea: Evidence from geochemical and palaeontological data. Palaeogeogr. Palaeocl. 177, 237-263. doi:10.1016/S0031-0182(01)00335-2.

Gorbarenko, S.A., Basov, I.A., Chekhovskaya, M.P., Southon, J., Khusid, T.A., Artemova, A.V., 2005. Orbital and millennium scale environmental changes in the southern Bering Sea during the last glacial-Holocene: Geochemical and paleontological evidence. Deep-Sea Res. Pt. II 52, 2174-2185. doi:10.1016/j.dsr2.2005.08.005.

Gorbarenko, S.A., Goldberg, E.L., Kashgarian, M., Velivetskaya, T.A., Zakharkov, S.P., Pechnikov, V.S., Bosin, A.A., Psheneva, O.Y., Ivanova, E.D., 2007. Millennium scale environment changes of the Okhotsk Sea during last 80 kyr and their phase relationship with global climate changes. J. Oceanogr. 63, 609-623.

Gorbarenko, S.A., Harada, N., Malakhov, M.I., Vasilenko, Y.P., Bosin, A.A., Goldberg, E.L., 2010a. Orbital and millennial-scale environmental and sedimentological changes in the Okhotsk Sea during the last 350 kyr. Global Planet. Change 72, 79-85. doi:10.1016/j.gloplacha.2010.03.002.

Gorbarenko, S.A., Wang, P., Wang, R., Cheng, X., 2010b. Orbital and suborbital environmental changes in the southern Bering Sea during the last 50 kyr. Palaeogeogr. Palaeocl. 286, 97-106. doi:10.1016/j.palaeo.2009.12.014.

Gorbarenko, S.A., Harada, N., Malakhov, M.I., Velivetskaya, T.A., Vasilenko, Y.P., Bosin, A.A., Derkachev, A.N., Goldberg, E.L., Ignatiev, A.V., 2012. Responses of the Okhotsk Sea environment and sedimentology to global climate changes at the orbital and millennial scale during the last 350 kyr. Deep-Sea Res. Pt. II 61-64, 73-84. doi:10.1016/j.dsr2.2011.05.016.

Guo, L., Macdonald, R.W., 2006. Source and transport of terrigenous organic matter in the upper Yukon River: Evidence, from isotopic ($\delta^{13}C$, $\Delta^{14}C$, and $\delta^{15}N$) composition of dissolved, colloidal, and particulate phases. Global Biogeochem. Cy. 20, GB2011. doi:10.1029/2005GB002593.

Guo, L., Tanaka, T., Wang, D., Tanaka, N., Murata, A., 2004. Distributions, speciation and stable isotope composition of organic matter in the southeastern Bering Sea. Mar. Chem. 91, 211-226. doi:10.1016/j.marchem.2004.07.002.

Haug, G.H., Sigman, D.M., Tiedemann, R., Pedersen, T.F., Sarnthein, M., 1999. Onset of permanent stratification in the subarctic Pacific Ocean. Nature 401, 779-782.

Hendy, I.L., Kennett, J.P., 2000. Dansgaard-Oeschger cycles and the California Current System: Planktonic foraminiferal response to rapid climate change in Santa Barbara Basin, Ocean Drilling Program hole 893A. Paleoceanography 15 (1), 30-42.

Hendy, I.L., Kennett, J.P., 2003. Tropical forcing of North Pacific intermediate water distribution during Late Quaternary rapid climate change? Quaternary Sci. Rev. 22, 673-689. doi:10.1016/S0277-3791(02)00186-5.

Honda, M.C., Imai, K., Nojiri, Y., Hoshi, F., Sugawara, T., Kusakabe, M., 2002. The biological pump in the northwestern North Pacific based on fluxes and major components of particulate matter obtained by sediment-trap experiments (1997-2000). Deep-Sea Res. Pt. II 49, 5595-5625. doi:10.1016/S0967-0645(02)00201-1.

Horikawa, K., Asahara, Y., Yamamoto, K., Okazaki, Y., 2010. Intermediate water formation in the Bering Sea during glacial periods: Evidence from neodymium isotope ratios. Geology 38 (5), 435-438. doi:10.1130/G30225.1.

Hu, A., Meehl, G.A., Otto-Bliesner, B.L., Waelbroeck, C., Han, W., Loutre, M.-F., Lambeck, K., Mitrovica, J.X., Rosenbloom, N., 2010. Influence of Bering Strait flow and North Atlantic circulation on glacial sea-level changes. Nat. Geosci. 3, 118-121. doi:10.1038/ngeo0729.

Itaki, T., Uchida, M., Kim, S., Shin, H.-S., Tada, R., Khim, B.-K., 2009. Late Pleistocene stratigraphy and palaeoceanographic implications in northern Bering Sea slope sediments: Evidence from the radiolarian species *Cycladophora davisiana*. J. Quaternary Sci. 24 (8), 856-865. doi:10.1002/jqs.1356.

Jaccard, S.L., Galbraith, E.D., 2012. Large climate-driven changes of oceanic oxygen concentrations during the last deglaciation. Nat. Geosci. 5 (2), 151-156. doi:10.1038ngeo1352.

Jaccard, S.L., Galbraith, E.D., 2013. Direct ventilation of the North Pacific did not reach the deep ocean during the last deglaciation. Geophys. Res. Lett. 40, 199-203. doi:10.1029/2012GL054118.

Jaccard, S.L., Haug, G.H., Sigman, D.M., Pedersen, T.F., Thierstein, H.R., Röhl, U., 2005. Glacial/interglacial changes in subarctic North Pacific stratification. Science 308, 1003-1006. doi:10.1126/science.1108696.

Jaccard, S.L., Galbraith, E.D., Sigman, D.M., Haug, G.H., 2010. A pervasive link between Antarctic ice core and subarctic Pacific sediment records over the past 800 kyrs. Quaternary Sci. Rev. 29, 206-212. doi:10.1016/j.quascirev.2009.10.007.

Kao, S.J., Liu, K.K., Hsu, S.C., Chang, Y.P., Dai, M.H., 2008. North Pacific-wide spreading of isotopically heavy nitrogen during the last deglaciation: Evidence from the western Pacific. Biogeosciences 5, 1641-1650. doi:10.5194/bg-5-1641-2008.

Kashiyama, Y., Ogawa, N.O., Shiro, M., Tada, R., Kitazato, H., Ohkouchi, N., 2008. Reconstruction of the biogeochemistry and ecology of photoautotrophs based on the nitrogen and carbon isotopic compositions of vanadyl porphyrins from Miocene siliceous sediments. Biogeosciences 5, 797-816. doi:10.5194/bg-5-797-2008.

Katsuki, K., Takahashi, K., 2005. Diatoms as paleoenvironmental proxies for seasonal productivity, sea-ice and surface circulation in the Bering Sea during the late Quaternary. Deep-Sea Res. Pt. II 52, 2110-2130. doi:10.1016/j.dsr2.2005.07.001.

Keigwin, L.D., Jones, G.A., Froelich, P.N., 1992. A 15,000 year paleoenvironmental record from Meiji Seamount, far northwestern Pacific. Earth Planet. Sc. Lett. 111, 425-440.

Keigwin, L.D., Donnelly, J.P., Cook, M.S., Driscoll, N.W., Brigham-Grette, J., 2006. Rapid sea-level rise and Holocene climate in the Chukchi Sea. Geology 34 (10), 861-864. doi:10.1130/G22712.1.

Khim, B.-K., Sakamoto, T., Harada, N., 2012. Reconstruction of surface water conditions in the central region of the Okhotsk Sea during the last 180 kyrs. Deep-Sea Res. Pt. II 61-64, 63-72. doi:10.1016/j.dsr2.2011.05.014.

Kienast, S.S., Calvert, S.E., Pedersen, T.F., 2002. Nitrogen isotope and productivity variations along the northeast Pacific margin over the last 120 kyr: Surface and subsurface paleoceanography. Paleoceanography 17 (4), 1055. doi:10.1029/2001PA000650.

Kienast, S.S., Hendy, I.L., Crusius, J., Pedersen, T.F., Calvert, S.E., 2004. Export production in the subarctic North Pacific over the last 800 kyrs: No evidence for iron fertilization? J. Oceanogr. 60 (1), 189-203.

Kim, S., Khim, B.K., Uchida, M., Itaki, T., Tada, R., 2011. Millennial-scale paleoceanographic events and implication for the intermediate-water ventilation in the northern slope area of the Bering Sea during the last 71 kyrs. Global Planet. Change 79, 89-98. doi:10.1016/j.gloplacha.2011.08.004.

Lam, P.J., Robinson, L.F., Blusztajn, J., Li, C., Cook, M.S., McManus, J.F., Keigwin, L.D., 2013. Transient stratification as the cause of the North Pacific productivity spike during deglaciation. Nat. Geosci. 6, 622-626. doi:10.1038/ngeo1873.

Laskar, J., Robutel, P., Joutel, F., Gastineau, M., Correia, A.C.M., Levrard, B., 2004. A long-term numerical solution for the insolation quantities of the Earth. Astron. Astrophys. 428, 261-285. doi:10.1051/0004-6361:20041335.

Lehmann, M.F., Sigman, D.M., McCorkle, D.C., Brunelle, B.G., Hoffmann, S., Kienast, M., Cane, G., Clement, J., 2005. Origin of the deep Bering Sea nitrate deficit: Constraints from the nitrogen and oxygen isotopic composition of water column nitrate and benthic nitrate fluxes. Global Biogeochem. Cy. 19, GB4005. doi:10.1029/2005GB002508.

Lisiecki, L.E., Raymo, M.E., 2005. A Pliocene-Pleistocene stack of 57 globally distributed benthic $\delta^{18}O$ records. Paleoceanography 20, PA1003. doi:10.1029/2004PA001071.

Liu, K.-K., Kaplan, I.R., 1989. The eastern tropical Pacific as a source of ^{15}N-enriched nitrate in seawater off southern California. Limnol. Oceanogr. 34 (5), 820-830.

Macdonald, A.M., Suga, T., Curry, R.G., 2001. An isopycnally averaged North Pacific climatology. J. Atmos. Ocean. Tech. 18 (3), 394-420.

Mariotti, A., Germon, J.C., Hubert, P., Kaiser, P., Letolle, R., Tardieux, A., Tardieux, P., 1981. Experimental determination of nitrogen kinetic isotope fractionation: Some principles; Illustration for the denitrification and nitrification processes. Plant Soil 62 (3), 413-430. doi:10.1007/BF02374138.

Matsumoto, K., Oba, T., Lynch-Stieglitz, J., Yamamoto, H., 2002. Interior hydrography and circulation of the glacial Pacific Ocean. Quaternary Sci. Rev. 21, 1693-1704. doi:10.1016/S0277-3791(01)00142-1.

Max, L., Riethdorf, J.-R., Tiedemann, R., Smirnova, M., Lembke-Jene, L., Fahl, K., Nürnberg, D., Matul, A., Mollenhauer, G., 2012. Sea surface temperature variability and sea-ice extent in the subarctic northwest Pacific during the past 15,000 years. Paleoceanography 27, PA3213. doi:10.1029/2012PA002292.

Max, L., Lembke-Jene, L., Riethdorf, J.-R., Tiedemann, R., Nürnberg, D., Kühn, H., Mackensen, A., 2014. Pulses of enhanced North Pacific Intermediate Water ventilation from the Okhotsk Sea and Bering Sea during the last deglaciation. Clim. Past 10, 591-605. doi:10.5194/cp-10-591-2014.

McQuoid, M.R., Whiticar, M.J., Calvert, S.E., Pedersen, T.F., 2001. A post-glacial isotope record of primary production and accumulation in the organic sediments of Saanich Inlet, ODP Leg 169S. Mar. Geol. 174, 273-286.

Méheust, M., Fahl, K., Stein, R., 2013. Variability in modern sea surface temperature, sea ice and terrigenous input in the sub-polar North Pacific and Bering Sea: Reconstruction from biomarker data. Org. Geochem. 57, 54-64. doi:10.1016/j.orggeochem.2013.01.008i.

Menviel, L., Timmermann, A., Elison Timm, O., Mouchet, A., Abe-Ouchi, A., Chikamoto, M.O., Harada, N., Ohgaito, R., Okazaki, Y., 2012. Removing the North Pacific halocline: Effects on global climate, ocean circulation and the carbon cycle. Deep-Sea Res. Pt. II 61-64, 106-113. doi:10.1016/j.dsr2.2011.03.005.

Meyers, P.A., 1994. Preservation of elemental and isotopic source identification of sedimentary organic matter. Chem. Geol. 114, 289-302.

Müller, P.J., Schneider, R., 1993. An automated leaching method for the determination of opal in sediments and particulate matter. Deep-Sea Res. Pt. I 40 (3), 425-444.

Nagashima, K., Asahara, Y., Takeuchi, F., Harada, N., Toyoda, S., Tada, R., 2012. Contribution of detrital materials from the Yukon River to the continental shelf sediments of the Bering Sea based on the electron spin resonance signal intensity and crystallinity of quartz. Deep-Sea Res. Pt. II 61-64, 145-154. doi:10.1016/j.dsr2.2011.12.001.

Nakatsuka, T., Watanabe, K., Handa, N., Matsumoto, E., 1995. Glacial to interglacial surface nutrient variations of Bering deep basins recorded by $\delta^{13}C$ and $\delta^{15}N$ of sedimentary organic matter. Paleoceanography 10 (6), 1047-1061.

Narita, H., Sato, M., Tsunogai, S., Murayama, M., Ikehara, M., Nakatsuka, T., Wakatsuchi, M., Harada, N., Ujiié, Y., 2002. Biogenic opal indicating less productive northwestern North Pacific during the glacial ages. Geophys. Res. Lett. 29 (15), 1732. doi:10.1029/2001GL014320.

Needoba, J.A., Waser, N.A., Harrison, P.J., Calvert, S.E., 2003. Nitrogen isotope fractionation in 12 species of marine phytoplankton during growth on nitrate. Mar. Ecol.-Prog. Ser. 255, 81-91. doi:10.3354/meps255081.

Niebauer, H.J., Bond, N.A., Yakunin, L.P., Plotnikov, V.V., 1999. An update on the climatology and sea ice of the Bering Sea, in: Loughlin, T.R., Ohtani, K. (Eds.), Dynamics of the Bering Sea. University of Alaska Sea Grant, Fairbanks, Alaska, pp. 29-59.

North Greenland Ice Core Project members, 2004. High-resolution record of Northern Hemisphere climate extending into the last interglacial period. Nature 431, 147-151. doi:10.1038/nature02848.

Nürnberg, D., Tiedemann, R., 2004. Environmental change in the Sea of Okhotsk during the last 1.1 million years. Paleoceanography 19, PA4011. doi:10.1029/2004PA001023.

Nürnberg, D., Dethleff, D., Tiedemann, R., Kaiser, A., Gorbarenko, S.A., 2011. Okhotsk Sea ice coverage and Kamchatka glaciation over the last 350 ka - Evidence from ice-rafted debris and planktonic $\delta^{18}O$. Palaeogeogr. Palaeocl. 310, 191-205. doi:10.1016/j.palaeo.2011.07.011.

Ohkushi, K., Itaki, T., Nemoto, N., 2003. Last Glacial-Holocene change in intermediate-water ventilation in the Northwestern Pacific. Quaternary Sci. Rev. 22, 1477-1484. doi:10.1016/S0277-3791(03)00082-9.

Okazaki, Y., Takahashi, K., Asahi, H., Katsuki, K., Hori, J., Yasuda, H., Sagawa, Y., Tokuyama, H., 2005a. Productivity changes in the Bering Sea during the late Quaternary. Deep-Sea Res. Pt. II 52, 2150-2162. doi:10.1016/j.dsr2.2005.07.003.

Okazaki, Y., Takahashi, K., Katsuki, K., Ono, A., Hori, J., Sakamoto, T., Uchida, M., Shibata, Y., Ikehara, M., Aoki, K., 2005b. Late Quaternary paleoceanographic changes in the southwestern Okhotsk Sea: Evidence from geochemical, radiolarian, and diatom records. Deep-Sea Res. Pt. II 52, 2332-2350. doi:10.1016/j.dsr2.2005.07.007.

Okazaki, Y., Timmermann, A., Menviel, L., Harada, N., Abe-Ouchi, A., Chikamoto, M.O., Mouchet, A., Asahi, H., 2010. Deepwater formation in the North Pacific during the last glacial termination. Science 329, 200-204. doi:10.1126/science.1190612.

Okazaki, Y., Sagawa, T., Asahi, H., Horikawa, K., Onodera, J., 2012. Ventilation changes in the western North Pacific since the last glacial period. Clim. Past 8, 17-24. doi:10.5194/cp-8-17-2012.

Ortiz, J.D., O'Connell, S.B., DelViscio, J., Dean, W., Carriquiry, J.D., Marchitto, T., Zheng, Y., van Geen, A., 2004. Enhanced marine productivity off western North America during warm climate intervals of the past 52 k.y.. Geology 32 (6), 521-524. doi:10.1130/G20234.1.

Ovsepyan, E.A., Ivanova, E.V., Max, L., Riethdorf, J.-R., Nürnberg, D., Tiedemann, R., 2013. Late Quaternary oceanographic conditions in the western Bering Sea. Oceanology 53 (2), 211-222. doi:10.1134/S0001437013020136.

Pennock, J.R., Velinsky, D.J., Ludlam, J.M., Sharp, J.H., Fogel, M.L., 1996. Isotopic fractionation of ammonium and nitrate during uptake by *Skeletonema costatum*: Implications for $\delta^{15}N$ dynamics under bloom conditions. Limnol. Oceanogr. 41 (3), 451-459.

Perdue, E.M., Koprivnjak, J.-F., 2007. Using the C/N ratio to estimate terrigenous inputs of organic matter to aquatic environments. Estuar. Coast. Shelf S. 73, 65-72. doi:10.1016/j.ecss.2006.12.021.

Rasmussen, S.O., Andersen, K.K., Svensson, A.M., Steffensen, J.P., Vinther, B.M., Clausen, H.B., Siggaard-Andersen, M.-L., Johnsen, S.J., Larsen, L.B., Dahl-Jensen, D., Bigler, M., Röthlisberger, R., Fischer, H., Goto-Azuma, K., Hansson, M.E., Ruth, U., 2006. A new Greenland ice core chronology for the last glacial termination. J. Geophys. Res. 111, D06102. doi:10.1029/2005JD006079.

Rella, S.F., Tada, R., Nagashima, K., Ikehara, M., Itaki, T., Ohkushi, K., Sakamoto, T., Harada, N., Uchida, M., 2012. Abrupt changes of intermediate water properties on the northeastern slope of the Bering Sea during the last glacial and deglacial period. Paleoceanography 27, PA3203. doi:10.1029/2011PA002205.

Riethdorf, J.-R., Nürnberg, D., Max, L., Tiedemann, R., Gorbarenko, S.A., Malakhov, M.I., 2013a. Millennial-scale variability of marine productivity of marine productivity and terrigenous matter supply in the western Bering Sea over the past 180 kyr. Clim. Past 9, 1345-1373. doi:10.5194/cp-9-1345-2013.

Riethdorf, J.-R., Max, L., Nürnberg, D., Lembke-Jene, L., Tiedemann, R., 2013b. Deglacial development of (sub) sea surface temperature and salinity in the subarctic northwest Pacific: Implications for upper-ocean stratification. Paleoceanography 28, 91-104. doi:10.1002/palo.20014.

Robinson, R.S., Kienast, M., Albuquerque, A.L., Altabet, M., Contreras, S., De Pol Holz, R., Dubois, N., Francois, R., Galbraith, E., Hsu, T.-C., Ivanochko, T., Jaccard, S., Kao, S.-J., Kiefer, T., Kienast, S., Lehmann, M.F., Martinez, P., McCarthy, M., Möbius, J., Pedersen, T., Quan, T.M., Ryabenko, E., Schmittner, A., Schneider, R., Schneider-Mor, A., Shigemitsu, M., Sinclair, D., Somes, C., Studer, A., Thunell, R., Yang, J.-Y., 2012. A review of nitrogen isotopic alteration in marine sediments. Paleoceanography 27, PA4203. doi:10.1029/2012PA002321.

Roden, G.I., 1995. Aleutian Basin of the Bering Sea: Thermohaline, oxygen, nutrient, and current structure in July 1993. J. Geophys. Res. 100 (C7), 13539-13554. doi:10.1029/95JC01291.

Roden, G.I., 2000. Flow and water property structures between the Bering Sea and Fiji in the summer of 1993. J. Geophys. Res. 105 (C12), 28595-28612. doi:10.1029/1999JC000030.

Sancetta, C., 1983. Effect of Pleistocene glaciation upon oceanographic characteristics of the North Pacific Ocean and Bering Sea. Deep-Sea Res 30 (8A), 851-869.

Sarnthein, M., Stattegger, K., Dreger, D., Erlenkeuser, H., Grootes, P., Haupt, B.J., Jung, S., Kiefer, T., Kuhnt, W., Pflaumann, U., Schäfer-Neth, C., Schulz, H., Schulz, M., Seidov, D., Simstich, J., van Kreveld, S., Vogelsang, E., Völker, A., Weinelt, M., 2001. Fundamental modes and abrupt changes in North Atlantic circulation and climate over the last 60 ky - Concepts, reconstruction and numerical modeling, in: Schäfer, P., Ritzrau, W., Schlüter, M., Thiede, J. (Eds.),The Northern North Atlantic: A Changing Environment, Springer, Berlin, pp. 365-410.

Schlitzer, R., 2013. Ocean Data View, http://odv.awi.de (last access: 4 February 2013).

Schlung, S.A., Ravelo, A.C., Aiello, I.W., Andreasen, D.H., Cook, M.S., Drake, M., Dyez, K.A., Guilderson, T.P., LaRiviere, J., Stroynowski, Z., Takahashi, K., 2013. Millennial-scale climate change and intermediate water circulation in the Bering Sea from 90 ka: A high-resolution record from IODP Site U1340. Paleoceanography 28, 1-14. doi:10.1029/2012PA002365.

Seki, O., Ikehara, M., Kawamura, K., Nakatsuka, T., Ohnishi, K., Wakatsuchi, M., Narita, H., Sakamoto, T., 2004. Reconstruction of paleoproductivity in the Sea of Okhotsk over the last 30 kyr. Paleoceanography 19, PA1016. doi:10.1029/2002PA000808.

Shigemitsu, M., Narita, H., Watanabe, Y.W., Harada, N., Tsunogai, S., 2007. Ba, Si, U, Al, Sc, La, Th, C and $^{13}C/^{12}C$ in a sediment core in the western subarctic Pacific as proxies of past biological production. Mar. Chem. 106, 442-455. doi:10.1016/j.marchem.2007.04.004.

Shigemitsu, M., Watanabe, Y.W., Narita, H., 2008. Time variations of $\delta^{15}N$ of organic nitrogen in deep western subarctic Pacific sediment over the last 145 ka. Geochem. Geophy. Geosy. 9 (10), Q10012. doi:10.1029/2008GC001999.

Sigman, D.M., Altabet, M.A., McCorkle, D.C., Francois, R., Fischer, G., 1999. The $\delta^{15}N$ of nitrate in the Southern Ocean: Consumption of nitrate in surface waters. Global Biogeochem. Cy. 13 (4), 1149-1166. doi:10.1029/1999GB900038.

Sigman, D.M., Altabet, M.A., McCorkle, D.C., Francois, R., Fischer, G., 2000. The $\delta^{15}N$ of nitrate in the Southern Ocean: Nitrogen cycling and circulation in the ocean interior. J. Geophys. Res. 105 (C8), 19599-19614.

Sigman, D.M., Lehman, S.J., Oppo, D.W., 2003. Evaluating mechanisms of nutrient depletion and ^{13}C enrichment in the intermediate-depth Atlantic during the last ice age. Paleoceanography 18 (3), 1072. doi:10.1029/2002PA000818.

Sigman, D.M., Hain, M.P., Haug, G.H., 2010. The polar ocean and glacial cycles in atmospheric CO_2 concentration. Nature 466, 47-55. doi:10.1038/nature09149.

Smith, S.L., Henrichs, S.M., Rho, T., 2002. Stable C and N isotopic composition of sinking particles and zooplankton over the southeastern Bering Sea shelf. Deep-Sea Res. Pt. II 49, 6031-6050. doi:10.1016/S0967-0645(02)00332-6.

Somes, C.J., Schmittner, A., Galbraith, E.D., Lehmann, M.F., Altabet, M.A., Montoya, J.P., Letelier, R.M., Mix, A.C., Bourbonnais, A., Eby, M., 2010. Simulating the global distribution of nitrogen isotopes in the ocean. Global Biogeochem. Cy. 24, GB4019. doi:10.1029/2009GB003767.

Springer, A.M., McRoy, C.P., Flint, M.V., 1996. The Bering Sea Green Belt: Shelf-edge processes and ecosystem production. Fish. Oceanogr. 5, 205-223.

Stabeno, P.J., Schumacher, J.D., Ohtani, K., 1999. The physical oceanography of the Bering Sea, in: Loughlin, T.R., Ohtani, K. (Eds.), Dynamics of the Bering Sea. University of Alaska Sea Grant, Fairbanks, Alaska, pp. 1-28.

Takahashi, K., Fujitani, N., Yanada, M., 2002a. Long term monitoring of particle fluxes in the Bering Sea and the central subarctic Pacific Ocean, 1990-2000. Progr. Oceanogr. 55, 95-112. doi:10.1016/S0079-6611(02)00072-1.

Takahashi, T., Sutherland, S.C., Sweeney, C., Poisson, A., Metzl, N., Tilbrook, B., Bates, N., Wanninkhof, R., Feely, R.A., Sabine, C., Olafsson, J., Nojiri, Y., 2002b. Global sea-air CO_2 flux based on climatological surface ocean pCO_2, and seasonal biological and temperature effects. Deep-Sea Res.. Pt. II 49, 1601-1622. doi:10.1016/S0967-0645(02)00003-6.

Tanaka, S., Takahashi, K., 2005. Late Quaternary paleoceanographic changes in the Bering Sea and the western subarctic Pacific based on radiolarian assemblages. Deep-Sea Res. Pt. II 52, 2131-2149. doi:10.1016/j.dsr2.2005.07.002.

Ternois, Y., Kawamura, K., Keigwin, L., Ohkouchi, N., Nakatsuka, T., 2001. A biomarker approach for assessing marine and terrigenous inputs to the sediments of Sea of Okhotsk for the last 27,000 years. Geochim. Cosmochim. Ac. 65 (5), 791-802.

Thunell, R.C., Sigman, D.M., Muller-Karger, F., Astor, Y., Varela, R., 2004. Nitrogen isotope dynamics of the Cariaco Basin, Venezuela. Global Biogeochem. Cy. 18, GB3001. doi:10.1029/2003GB002185.

Tomczak, M., Godfrey, J.S., 1994. Regional oceanography: An introduction. Elsevier Science Ltd., Oxford, 391 pp.

Tsuda, A., Takeda, S., Saito, H., Nishioka, J., Nojiri, Y., Kudo, I., Kiyosawa, H., Shiomoto, A., Imai, K., Ono, T., Shimamoto, A., Tsumune, D., Yoshimura, T., Aono, T., Hinuma, A., Kinugasa, M., Suzuki, K., Sohrin, Y., Noiri, Y., Tani, H., Deguchi, Y., Tsurushima, N., Ogawa, H., Fukami, K., Kuma, K., Saino, T., 2003. A mesoscale iron enrichment in the western subarctic Pacific induces a large centric diatom bloom. Science 300, 958-961. doi:10.1126/science.1082000.

Tyrrell, T., Merico, A., Waniek, J.J., Wong, C.S., Metzl, N., Whitney, F., 2005. Effect of seafloor depth on phytoplankton blooms in high-nitrate, low-chlorophyll (HNLC) regions. J. Geophys. Res. 110, G02007. doi:10.1029/2005JG000041.

van Geen, A., Zheng, Y., Bernhard, J.M., Cannariato, K.G., Carriquiry, J., Dean, W.E., Eakins, B.W., Ortiz, J.D., Pike, J., 2003. On the preservation of laminated sediments along the western margin of North America. Paleoceanography 18 (4), 1098. doi:10.1029/2003PA000911.

VanLaningham, S., Pisias, N.G., Duncan, R.A., Clift, P.D., 2009. Glacial-interglacial sediment transport to the Meiji Drift, northwest Pacific Ocean: Evidence for timing of Beringian outwashing. Earth Planet. Sc. Lett. 277, 64-72. doi:10.1016/j.epsl.2008.09.033.

Waelbroeck, C., Labeyrie, L., Michel, E., Duplessy, J.C., McManus, J.F., Lambeck, K., Balbon, E., Labracherie, M., 2002. Sea-level and deep water temperature changes derived from benthic foraminifera isotopic records. Quaternary Sci. Rev. 21, 295-305. doi:10.1016/S0277-3791(01)00101-9.

Walinsky, S.E., Prahl, F.G., Mix, A.C., Finney, B.P., Jaeger, J.M., Rosen, G.P., 2009. Distribution and composition of organic matter in surface sediments of coastal Southeast Alaska. Cont. Shelf Res. 29, 1565-1579. doi:10.1016/j.csr.2009.04.006.

Walsh, E.M., Ingalls, A.E., Keil, R.G., 2008. Sources and transport of terrestrial organic matter in Vancouver Island fjords and the Vancouver-Washington Margin: A multiproxy approach using $\delta^{13}C_{org}$, lignin phenols, and the ether lipid BIT index. Limnol. Oceanogr. 53 (3), 1054-1063. doi:10.4319/lo.2008.53.3.1054.

Wang, Y., Cheng, H., Edwards, R.L., Kong, X., Shao, X., Chen, S., Wu, J., Jiang, X., Wang, X., An, Z., 2008. Millennial- and orbital-scale changes in the East Asian monsoon over the past 224,000 years. Nature 451, 1090-1093. doi:10.1038/nature06692.

Warren, B.A., 1983. Why is no deep water formed in the North Pacific? J. Mar. Res. 41, 327-347.

Waser, N.A.D., Harrison, P.J., Nielsen, B., Calvert, S.E., Turpin, D.H., 1998. Nitrogen isotope fractionation during the uptake and assimilation of nitrate, nitrite, ammonium, and urea by a marine diatom. Limnol. Oceanogr. 43 (2), 215-224.

Yamamoto, M., Tanaka, N., Tsunogai, S., 2001. Okhotsk Sea intermediate water formation deduced from oxygen isotope systematics. J. Geophys. Res. 106 (C12), 31075-31084.

Yasuda, I., 1997. The origin of the North Pacific Intermediate Water. J. Geophys. Res. 102 (C1), 893-909.

Yokoyama, Y., Esat, T.M., 2011. Global climate and sea level: Enduring variability and rapid fluctuations over the past 150,000 years. Oceanography 24 (2), 54-69. doi:10.5670/oceanog.2011.27.

Zhang, J., Woodgate, R., Moritz, R., 2010. Sea ice response to atmospheric and oceanic forcing in the Bering Sea. J. Phys. Oceanogr. 40 (8), 1729-1747. doi:10.1175/2010JPO4323.1.

Zheng, Y., van Geen, A., Anderson, R.F., Gardner, J.V., Dean, W.E., 2000. Intensification of the northeast Pacific oxygen minimum zone during the Bölling-Alleröd warm period. Paleoceanography 15 (5), 528-536.

Ziegler, M., Jilbert, T., de Lange, G.J., Lourens, L.J., and Reichart, G.-J. (2008), Bromine counts from XRF scanning as an estimate of the marine organic carbon content of sediment cores, Geochemistry Geophysics Geosystems, 9(5), Q05009, doi:10.1029/2007GC001932.

Figure captions

Figure 1: (a) Surface circulation pattern (red arrows; after Tomczak and Godfrey, 1994; Stabeno et al., 1999) and bathymetry of the subarctic North Pacific realm. The red dot marks the location of sediment core SO201-2-85KL studied here. Published reference records are marked by yellow dots. Bering Sea: MR06-04-PC24A (Kim et al., 2011), KH99-3-BOW-8A (Horikawa et al., 2010), HLY02-02-17JPC (Brunelle et al., 2007, 2010), IODP Site U1340 (Schlung et al., 2013). Okhotsk Sea: YK0712-GC9A (Khim et al., 2012), GGC27 (Brunelle et al., 2010). NW Pacific: MD01-2416

(Galbraith et al., 2008a), PC13 (Brunelle et al., 2010). NE Pacific: ODP Site 887 (Galbraith et al., 2008a). The modern average maximum sea-ice extent during March is indicated by the dashed black line (after Niebauer et al., 1999; Zhang et al., 2010; IRI/LDEO Climate Data Library, http://iridl.ldeo.columbia.edu/). Surface currents: ANSC = Aleutian North Slope Current, BSC = Bering Slope Current, EKC = East Kamchatka Current, ESC = East Sakhalin Current, NOC = North Okhotsk Current, SC = Soya Current, WKC = West Kamchatka Current. Straits: bus = Bussol Strait, kss = Kruzenshtern Strait, ks = Kamchatka Strait, ns = Near Strait, bp = Buldir Pass, as = Amchitka Strait, ap = Amukta Pass, up = Unimak Pass, bs = Bering Strait. (b) Surface nitrate concentration during modern summer (July-September; in µmol l^{-1}) from World Ocean Atlas 2009 data (Garcia et al., 2010). Maps produced with "Ocean Data View" (Schlitzer, 2013).

Figure 2: (a) Relationship between concentrations of total nitrogen (TN) and total organic carbon (TOC) in samples from core SO201-2-85KL. For the calculation of molar N/C ratios a linear regression between TOC and TN was used to assess the fraction of inorganic nitrogen, represented by the intercept of the regression line at TOC = 0. (b) Comparison with $\delta^{15}N_{bulk}$ indicates that there is only a weak linear relationship between the isotopic signal and TN concentrations ($R^2 = 0.24$; $p < 10^{-4}$).

Figure 3: Linear sedimentation rate (LSR) vs. bulk accumulation rate (AR Bulk), and comparison of concentration and accumulation rate (AR) records of Siliciclastics, $CaCO_3$, TOC and opal for core SO201-2-85KL.

Figure 4: Records reflecting changes in export production and terrigenous matter supply in core SO201-2-85KL over the past 180 kyr in comparison with Northern Hemisphere summer (July-September) insolation at 65°N (after Laskar et al., 2004). Logging data (underlying grey lines), %Siliciclastics, as well as $CaCO_3$ and opal concentrations are from Max et al. (2012) and Riethdorf et al. (2013a, 2013b). Note inverted axes of %Siliciclastics and XRF Al count rates. The $\delta^{18}O$ records from the

NGRIP ice core in Greenland (NGRIP members, 2004; GICC05 timescale, Rasmussen et al., 2006) and from the Sanbao stalagmites in China (Wang et al., 2008) are shown for reference. Greenland interstadials (GI) are highlighted by pale red vertical bars. Boundaries of Marine Isotope Stages (MIS) after Lisiecki and Raymo (2005).

Figure 5: Comparison of $\delta^{13}C_{bulk}$ with (a) molar N/C ratios and (b) $\delta^{15}N_{bulk}$ for core SO201-2-85KL. Samples from warm intervals (MIS 5.5, 5.3, 5.1, 3, and 1) are marked by red dots, while blue dots mark those from cold intervals (MIS 6, 5.4, 5.2, 4, 2), and green triangles indicate Holocene (<11.7 ka BP) samples. Grey-shaded boxes represent geochemical provenances (after literature data; see text for references). The dashed lines indicate the applied linear mixing model for the estimation of m_{terr}. Marine phytoplankton and vascular plant detritus (VPD) are considered as potential marine and terrestrial organic matter sources (endmembers).

Figure 6: Proxy records from core SO201-2-85KL in comparison with published reference records covering the last 180 kyr: (a) Northern Hemisphere summer (65°; July-September) insolation after Laskar et al. (2004), (b) sedimentary $\delta^{13}C$ and (c) molar N/C ratios used to estimate the fraction of terrestrial organic matter (m_{terr}; respective axes apply to those of $\delta^{13}C$ and N/C), (d) color b* assumed to reflect export production, (e) $\delta^{15}N_{bulk}$ reflecting surface nitrate utilization, (f) neodymium isotope ratios from core KH99-3-BOW-8A (Horikawa et al., 2010; cf. Figure 1) considered to approximate intermediate water formation, and (g) relative sea-level (Waelbroeck et al., 2002) normalized to the sill depth (~50 m; dashed line) of the Bering Strait (ΔRSL). MIS boundaries after Lisiecki and Raymo (2005), GI highlighted by pale red vertical bars.

Figure 7: Comparison of $\delta^{15}N_{bulk}$ from SO201-2-85KL (black line) with other sedimentary (solid lines) and diatom-bound (dotted lines) $\delta^{15}N$ records from the

subarctic North Pacific and its marginal seas (cf. Figure 1). The timing of Greenland interstadials and MIS boundaries are indicated.